tional to the part excited by electrons with the primary energy. This situation is more severe than in the case of the transmission experiment of Hall (1966). Under the experimental conditions of the Bragg case with a thick crystal, multiple processes of inelastic electron scattering continue until electrons wholly lose their energy in the crystal, and the integration of X-rays excited in the course of these processes inevitably makes a high background. In the case of a transmission experiment, on the other hand, the multiple process ceases when electrons emerge from a crystal which is very thin. As has already been pointed out, it should be profitable to use incident electrons of lower energies, say 10–20 keV, for the purpose of the present study. However, some other experimental difficulties will then arise.

References

ANNAKA, S. (1967). *J. Phys. Soc. Japan*, **23**, 372.
ANNAKA, S., KIKUTA, S. & KOHRA, K. (1966). *J. Phys. Soc. Japan*, **21**, 1559.
BATTERMAN, B. W. (1962). *Appl. Phys. Letters*, **1**, 68.
BATTERMAN, B. W. (1964). *Phys. Rev.* **133**, A 759.
BETHE, H. (1928). *Ann. Phys. Lpz.* **87**, 55.
BETHE, H. (1930). *Ann. Phys. Lpz.* **5**, 225.
DARWIN, C. G. (1914). *Phil. Mag.* **27**, 325, 675.
DUNCUMB, P. (1962). *Phil. Mag.* **7**, 2101.
EWALD, P. P. (1917). *Ann. Phys. Lpz.* **54**, 519, 577.
HALL, C. R. (1966). *Proc. Roy. Soc.* **295**, 140.
HIRSCH, P. B., HOWIE, A. & WHELAN, M. J. (1962). *Phil. Mag.* **7**, 2095.
JAMES, R. W. (1963). *Solid State Physics* (Edited by Seitz & Turnbull), **15**, 55.
KIKUCHI, K. & NAKAGAWA, S. (1933). *Sci. Pap. Inst. Phys. Chem. Res. Tokyo*, **21**, 256.
KNOWLES, J. W. (1956). *Acta Cryst.* **9**, 61.
KOHRA, K. & SHINOHARA, K. (1948). *J. Phys. Soc. Japan*, **4**, 155, 160.
KOHRA, K., MOLIÈRE, NAKANO, S. & ARIYAMA, M. (1962). *J. Phys. Soc. Japan*, **17**. Suppl. B-II, 82.
LAUE, M. (1960). *Röntgenstrahlinterferenzen*, 3rd edition. Akademische Verlag: Frankfurt a.M.
MIYAKE, S., HAYAKAWA, K. & MIIDA, R. (1966). *J. Phys. Soc. Japan*, **22**, 670.
MIYAKE, S., KOHRA, K. & TAKAGI, M. (1954). *Acta Cryst.* **7**, 393.
MIYAKE, S. (1962). *J. Phys. Soc. Japan*, **17**, 1642.
NIEHRS, H. (1959). *Z. Phys.* **156**, 446.
TAKAGI, S. (1958). *J. Phys. Soc. Japan*, **13**, 287.
ZACHARIASEN, W. H. (1945). *Theory of X-ray Diffraction in Crystals*. New York: John Wiley.

Acta Cryst. (1968). A **24**, 191

Multiple Diffraction Origin of Low Energy Electron Diffraction Intensities*

BY A. GERVAIS, R. M. STERN AND M. MENES

Department of Physics, Polytechnic Institute of Brooklyn, Brooklyn, N.Y., U.S.A.

(*Received* 9 *June* 1967)

The angular and voltage dependence of the diffracted intensity for electrons in the energy range of 150–900 volts from a clean tungsten (110) surface has been measured with a single-crystal diffractometer. Selecting the angle of incidence and the electron wavelength to satisfy the Bragg condition the crystal is rotated about its normal, and a Renninger plot of diffracted intensity *versus* azimuthal angle is made. Strong intensity variations are observed when the plane of diffraction is parallel to those low index crystallographic planes which contain relatively dense atomic rows. Additional structure occurs for each intersection of an extended reciprocal lattice point with the Ewald sphere. For some orientations the intensity is reduced to half the value within one degree, which is the beam divergence. When simultaneous diffraction does not occur, the intensities of the Bragg maxima are close to the background. The integral order Bragg maxima observed in electron diffraction are thus shown to have their origin in multiple diffraction. The frequently observed fractional order Bragg maxima are predicted to have the same origin. Renninger plots for such maxima show this to be the case. In addition the appearance of the fractional order peaks should depend only on the geometry for multiple diffraction. Intensity *versus* voltage curves for the beam incident along the [*hkl*] direction are predicted to have maxima of order $(h^2+k^2+l^2)^{-1}$, which is verified. The implication of these observations in terms of previous two-beam models is discussed.

Introduction

Much interest has recently been shown in obtaining a suitable theory for the diffraction of low energy electrons by single crystals. The solution of a model containing the formalism for all dynamic interactions possible is quite forbidding and it is necessary to decide, in advance, which processes must be included in a theory which is expected to allow a quantitative interpretation of diffracted intensities. An examination of the literature of electron diffraction will show that there is little agreement as to the importance of dynamical

* Supported by AFOSR Contract AF 49 (638)-1369.

effects at all, and much interpretation of experimental results has been made on the basis of kinematical theory alone; as a result, the angular and wavelength dependence of the diffracted intensities appears to be anomalous, and there has yet to be a three-dimensional structure determined by low energy electron diffraction. The purpose of this communication is to show, at least for the case of tungsten, that dynamic effects dominate the observed diffraction intensities, and to propose a model of the diffraction which allows a selection of the important dynamic processes.

The approach to be followed is that common in X-ray diffraction analysis, which provides a convenient geometry for both the experiments themselves, and the interpretation of the results in terms of general diffraction parameters. The fact that one deals with electrons, rather than X-rays, does not affect the geometry at all, but does require the introduction of a particular set of useful approximations, and appropriate experimental restrictions.

Geometrical considerations

Reciprocal lattice

The standard Ewald construction provides a method of determining the geometrically allowed reflections for a given lattice, as a function of arbitrary electron wavelength, λ, diffraction angle, θ, and crystal orientation (Ewald, 1921; James, 1962). An additional parameter, φ, can be introduced which determines the orientation of the incident plane with respect to a particular plane in the same zone defined as the origin. In the experiments described below, the crystal is cut and oriented so that the surface is the (110) plane, the surface normal is then the [110] direction, and the reference plane belongs to the {110} zone.

For arbitrary λ, θ, φ, the three Laue conditions are not in general satisfied. When the crystal lattice is composed of only a few biperiodic planes, the resulting reciprocal lattice consists of a set of rods perpendicular to these planes, and solutions to the two Laue conditions always exist. The intensity along these reciprocal lattice rods has a modulation (in the z direction) given by the term:

$$\left(\frac{\mathbf{S}-\mathbf{S}_0}{\lambda}\right) . Z_i$$

in the structure factor F_{hk}:

$$F_{hk} = \sum_i f_i \exp\left\{2\pi i \left[h\mathbf{x}_i + k\mathbf{y}_i + \left(\frac{\mathbf{S}-\mathbf{S}_0}{\lambda}\right) . Z_i\right]\right\}.$$

For the following discussion, it is sufficient to describe the reciprocal lattice in terms of these modulated rods, where the intensity along a rod has a maximum at the expected three-dimensional lattice points, and is non-zero elsewhere; the origin and exact nature of the modulation being unimportant.

In the case of X-ray diffraction, the reciprocal lattice is explored by observing the variation in intensity of the specularly reflected beam at constant wavelength as the angle of reflection, θ, is varied. In principle, the same information may be obtained by varying the wavelength, λ, maintaining θ constant, a more convenient choice of independent variable in the case of electron diffraction. Both θ and λ may be seen to be equivalent parameters in the kinematical limit, and the resulting intensity variations may both be considered to be rocking curves. The diffraction conditions are fulfilled at each intersection of the sphere of reflection with an allowed reciprocal lattice rod or point, and the rocking curves show Bragg maxima for the cor-

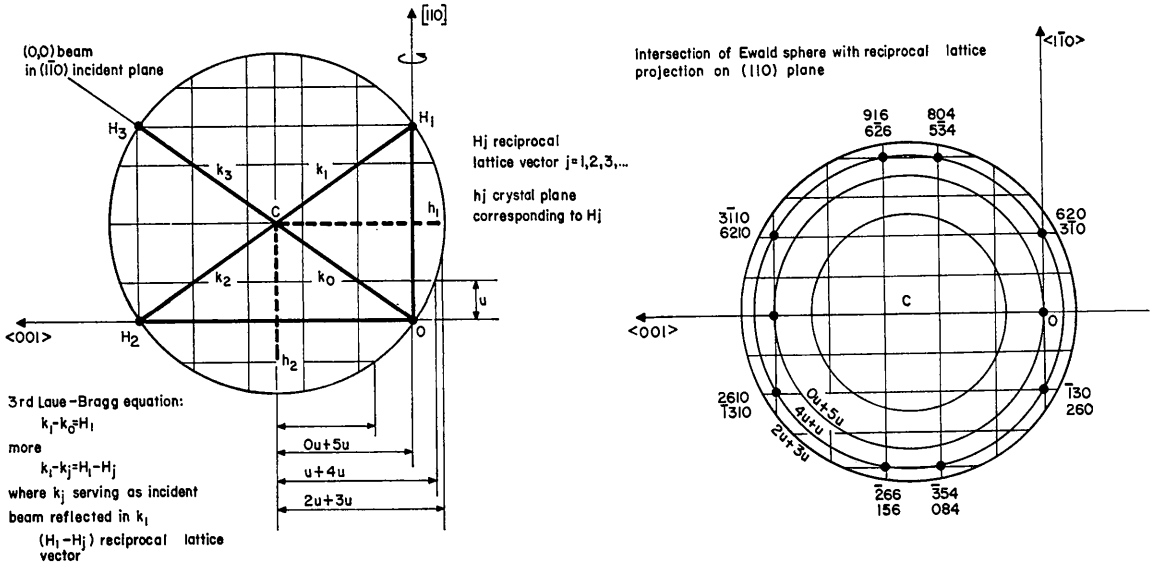

Fig. 1. Standard construction showing simultaneous beams occurring in a (110) orientation of the diffraction plane. The right hand diagram shows the projection of horizontal sections through the sphere of reflection indicating some of the other reflections. This geometry corresponds to about 500 volts for tungsten.

responding values of the diffraction parameters λ_B and θ_B, thus defined. This requirement is fulfilled independent of the orientation, φ, of the incident beam.

The details of this construction can be seen in Fig. 1, where the plane of diffraction is chosen as (110) and the surface normal is in the [110] direction. The left hand diagram shows the intersection of the sphere of reflection with the (110) plane of the reciprocal lattice, the specularly reflected beam showing the (550) reflection. It can be readily seen that both types of rocking curve (intensity *versus* θ and intensity *versus* voltage), explore the shape of the reciprocal lattice rod. The right hand diagram shows the projection on the (110) plane of the intersections of the Ewald sphere with the reciprocal lattice. Each successive plane parallel to the surface has the circular intersection shown, and passes through successive points $(n,n,0)$ of the (110) rod. The plane among these passing through the origin is known as the 0-Laue plane.

Rotation method

From Fig. 1 it may be seen that for any λ_B and θ_B, the crystal can be rotated about its normal without affecting the diffraction condition imposed on λ_B and θ_B. During the rotation the reciprocal lattice moves with respect to the sphere: in Fig. 1, the lattice moves with respect to the circles representing the intersection of each succeeding $(n,n,0)$ plane with the sphere. Two points, the origin and the normal Bragg reflection, in this case 550, remain fixed and define the axis of rotation.

If the intensity of the normally reflected beam is recorded during the rotation, any variation must be due to the dynamical interaction of other diffracted beams within the crystal with the specularly reflected beam. A plot of the intensity *versus* the rotation angle φ is known as a rotation diagram or Renninger plot.

For the three-dimensional reciprocal point lattice, each reciprocal lattice point is recorded as it enters the sphere of reflection. The existence of several simultaneous intersections is known as multiple diffraction* as discussed by Renninger (1937), Darbyshire & Cooper (1935), and Kossel (1936). The geometrical argument for multiple diffraction may be seen by referring to Fig. 1. If $\mathbf{k}_0$ is the wave vector of the primary beam, then $\mathbf{k}_t=\mathbf{k}_0+\mathbf{H}_t$, where $\mathbf{H}_t$ is a reciprocal lattice vector. In this case, $\mathbf{k}_t$ corresponds to a reflection if $\mathbf{H}_t$ is on the sphere of reflection. If simultaneous reflections $\mathbf{H}_1, \mathbf{H}_2 \ldots \mathbf{H}_j$ exist, then the set of simultaneous equations $\mathbf{k}_1=\mathbf{k}_0+\mathbf{H}_1, \mathbf{k}_2=\mathbf{k}_0+\mathbf{H}_2 \ldots \mathbf{k}_j=\mathbf{k}_0+\mathbf{H}_j$ exists. In particular, $\mathbf{k}_1=\mathbf{k}_2+(\mathbf{H}_1-\mathbf{H}_2)$, where $(\mathbf{H}_1-\mathbf{H}_2)$ is also a reciprocal lattice vector. In this case, $\mathbf{k}_2$ acts as a primary beam reflecting from the planes corresponding to the vector $(\mathbf{H}_1-\mathbf{H}_2)$, in the direction of the beam $\mathbf{k}_1$ and *vice versa*. For simultaneous diffraction, each diffracted beam will contribute to the intensity of all other diffracted beams occurring at the same time. One can generalize this statement by indicating that the intensity of the reflection $\mathbf{H}_1$ may be either increased by contributions from all the other beams or decreased by the propagation of energy in directions other than $\mathbf{k}_1$ and the introduction of new extinction paths. The net effect depends on the strength of the reflection $\mathbf{H}_1$ and the relative strength of all the other reflections, which depends on the magnitude of the vector $(\mathbf{H}_1-\mathbf{H}_2)$.

It should be pointed out that if the value of the reflection $\mathbf{H}_1$ is identically zero because the reflection is forbidden by the crystal lattice, then there is no mechanism by which multiple diffraction can place intensity in the direction $\mathbf{k}_1$. If on the other hand the reflected intensity $\mathbf{H}_1$ is zero because of the structure factor, but $\mathbf{H}_1$ is still allowed by the lattice, then the effect of the dynamical interaction will be to place intensity in the direction $\mathbf{k}_1$. This latter condition is what is usually referred to as the Renninger effect.

If the number of such simultaneous reflections is small, then standard X-ray techniques can be used to compute the relative diffraction intensities. A quantitative treatment of this problem has been made for both the case of X-rays and high energy electron diffraction (Saccocio & Zajac, 1965; Zachariasen, 1965).

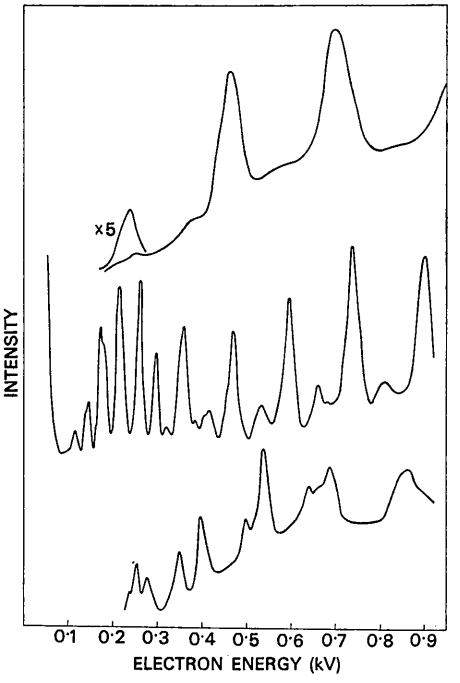

Fig. 2. Intensity *versus* voltage curves for the specularly reflected beam. Upper curve: [100] direction, $2\theta=90°$; middle curve: [110] direction, $2\theta=180°$; lower curve: [111] direction, $2\theta=70°32'$. The large peaks occur at voltages near to the expected integral order Bragg reflections, and the fractional order peaks correspond to $1/(h^2+k^2+l^2)$ of the integral order peak separation.

* It should be pointed out that several recent theoretical treatments of the dynamical diffraction problem contain implicitly the geometry of multiple diffraction. See, *e.g.* Boudreaux & Heine (1967), Kambe (1967), McRae (1966), Tournaire (1962).

The solution of the set of simultaneous equations involves knowledge of the polarization factor for each beam resulting in $2n+1$ equations for n simultaneous beams. The polarization of electrons by atomic scattering has recently been investigated (Bunyan & Schonfelder, 1965; Deichsel & Reichert, 1965; Deichsel, Reichert & Steidl, 1966; Loth & Eckstein, 1966; Steidl, Deichsel & Reichert, 1965) and very large values for the polarization for particular angles and voltages reported.*

Experimental observations

A single-crystal plate of tungsten, with a principal surface normal oriented to within 0·02° of the [110] direction, is mounted in a diffractometer placed in an ultra high vacuum system. This double crystal diffractometer, designed for the polarization experiments, will be described in detail elsewhere. In principle it permits the continuous rotation of the first crystal about its normal, at fixed diffraction angle. For the measurements described here, the second crystal is replaced by an electrostatic mirror, the current being measured by a Faraday cage placed in the reflecting position with respect to the mirror. A second Faraday cage having poor energy resolution (5 eV compared with about 1 eV) may be positioned in the beam after reflection from the first crystal, and is used as a rough check on the measurements. An identical crystal prepared in the same way is mounted in a standard post accelerated diffraction camera. The two crystals receive the same treatment, being heated to 2000 °C at 10^{-6} torr oxygen, until the crystal in the diffraction system exhibits a diffraction pattern associated with a clean surface.

Fig. 2 shows intensity *versus* voltage rocking curves from these crystals for several well defined orientations of the incident beam direction; *i.e.* φ and θ remain fixed for each curve. The most striking feature of these curves is the fact that the fractional orders observed depend on the direction of the incident beam. The curves have strong non-integral orders given by $1/(h^2+k^2+l^2)$ for the cases studied, and those of Fig. 2 show the intensity variation for the three directions of highest symmetry only. For arbitrary orientation the rocking curves in this energy range show three types of characteristic anomalies: the intensity maxima are shifted from the normal Bragg position; the intensity maxima are occasionally split; non-integer orders are always present.

The first two of these features are also observed in high energy electron diffraction and can be explained by a dynamic theory which treats the interaction between simultaneous waves. Non-integer orders are strictly forbidden by a three-dimensional reciprocal lattice, and are not observed in either high energy electron or X-ray diffraction. The presence of fractional order maxima implies that the reciprocal lattice must be extended for the case of electron diffraction in the energy range considered here. A possible origin for this extension will be discussed later.

Fig. 3 shows the rotation diagram for the specularly reflected beam when the rocking curve exhibits the integral order Bragg maximum shown in Fig. 1. In this case, $2\theta=65°$, the accelerating potential is 595 volts, and the specularly reflected beam exhibits the 550 reflection, about which the rotation is made. At relatively high voltages, that is for the 440, 550, 660, 770 reflections (Figs. 3, 4, and 5), each rotation diagram is characterized by strong positive intensity variations due to the changing conditions for multiple diffraction.

* The following rotation diagrams are the first results of a program to study the polarization of electrons by diffraction. If the polarization factor is known in detail, the problem of the diffracted intensities based on a multiple diffraction model can in principle be solved. The occurrence of multiple diffraction itself indicates that the direct measurement of the polarization will be difficult. The results of the polarization measurements will be published elsewhere. The first attempt to measure the polarization of electrons by a double crystal diffractometer was by Davisson & Germer (1929).

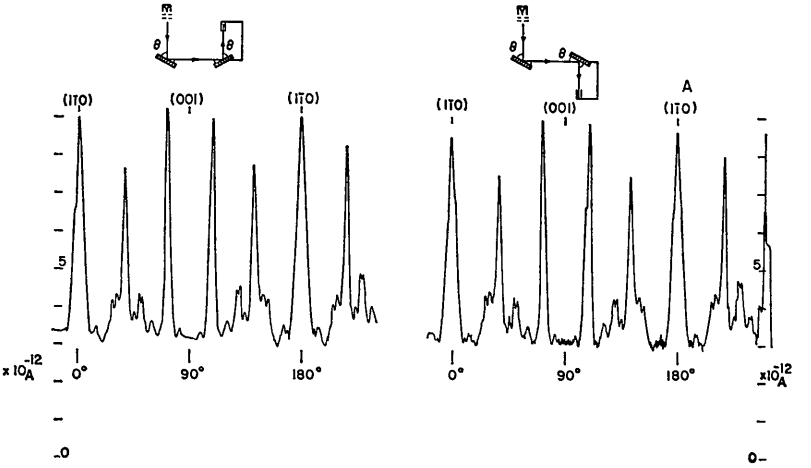

Fig. 3. Rotation diagram for $2\theta=65°$, 595 volts, about the 550 reflection. Made in the double scattering mode with the second crystal replaced by a mirror. The two curves are for parallel and antiparallel orientation of the second scattering geometry and exhibit no instrumental asymmetry.

As the diffraction angle or the wavelength is varied, the general character of the rotation diagrams does not change, except that as the volume of reciprocal space swept out by the sphere of reflection increases with increasing energy the number of maxima observed during a rotation increases accordingly (see Figs. 3 and 4). For the 330 reflection shown in Fig. 6 the character of the rotation diagram changes; strong negative multiple diffraction contributions appearing in the specularly reflected beam.

The lower curve in Fig. 7 shows the number (density) of simultaneous reflections as a function of rotation angle for the 550 reflection. The position of the structure in the rotation diagram is found to agree well with the position of the structure in the density plot, although there is little or no correlation between the reflected intensity and the number of simultaneous reflections, except for the (110) orientation.

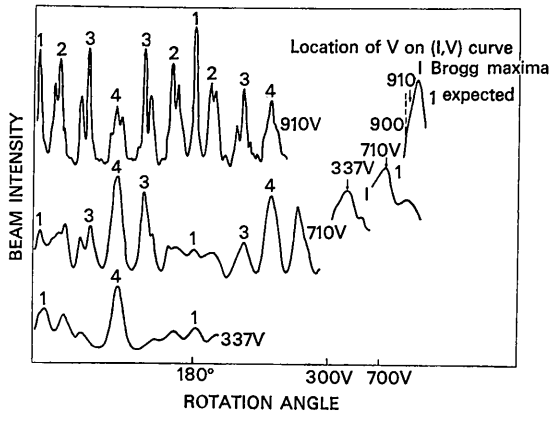

Fig. 4. Rotation diagram for several diameters of the sphere of reflection at constant diffraction angle, $2\theta=90°$. Upper curve 880 reflection (910 eV), middle curve 770 reflection (710 eV) lower curve 550 reflection (337 eV). The right hand diagrams show the intensity *versus* voltage curve near each reflection, for the (110) orientation.

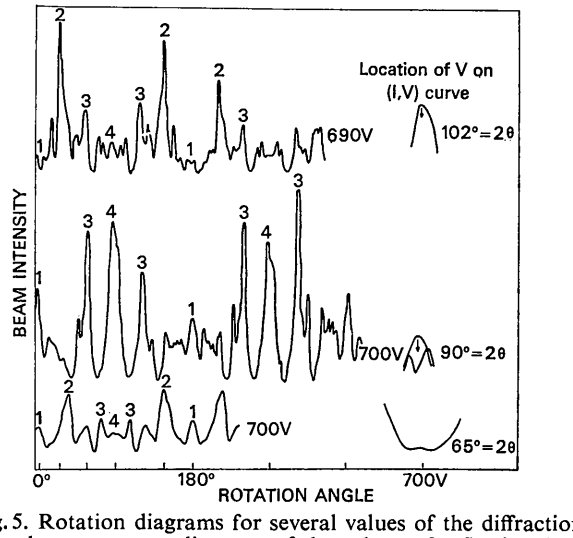

Fig. 5. Rotation diagrams for several values of the diffraction angle, at constant diameter of the sphere of reflection (700 volts). Upper curve $2\theta=102°$, middle curve $2\theta=90°$, lower curve $2\theta=65°$. At glancing angles there appears to be less structure in the diagram.

In Figs. 3, 4 and 5 the normal reflection from the crystal is particularly strong for the following orientations:

$2\theta=65°$;
(001), (1$\bar{1}$4), (1$\bar{1}$3), (1$\bar{1}$2), (1$\bar{1}$1), (2$\bar{2}$1), (3$\bar{3}$1), (1$\bar{1}$0),
$2\theta=90°$;
(001), (1$\bar{1}$4), (1$\bar{1}$3), (1$\bar{1}$2), (1$\bar{1}$1), (3$\bar{3}$2), (2$\bar{2}$1), (1$\bar{1}$0).

The low index diffraction planes which determine the orientation for the strong reflections are all characterized by having low index rows contained in the plane. Although the significance of this fact in the determination of the diffracted intensity is not known, it is observed that the angle between the direction of the diffraction beam and the direction of such a row is important. The crystal is found to exhibit an anomalously large reflection coefficient when the electron current (the equivalent of the Poynting vector for the X-ray case) is parallel to the closely spaced directions of the periodic crystal potential. Several of these directions correspond to the orientations of the Kikuchi bands observed for tungsten at high accelerating voltages (1500–2000 eV) (Stern & Baudoing, 1967). DeBersuder (1967) has been able to correlate the very broad structure of the rotation diagrams for aluminum with the presence of strong Kikuchi bands and lines, which in this case persist to much lower voltages.

Interpretation of the angular dependence of diffraction intensities

Crystal potential and the dynamical theory

A convenient description of an elastic model of multiple electron diffraction may be found in the dynamical theory due to Bethe (1928), which introduces the Fourier transform of the periodic lattice in terms of the periodic crystal potential V_r

$$V_r=\sum_h V_h \exp(2\pi i\mathbf{h}\cdot\mathbf{r}) \qquad (1)$$

as a perturbation on the electron wave functions in the crystal. Here $\mathbf{h}$ is a reciprocal lattice vector and h represents the triple index: a complete description may be found in Ziman (1960, 1964).

The amplitude of the electron wave, ψ_h, diffracted into a reflection h, is given to a first approximation by

$$\psi_h=\varphi_h+\sum_{h'}{}' \frac{V_{h-h'}\varphi_{h'}}{\hbar^2[\mathbf{k}^2-\mathbf{k}'^2]/2m} \qquad (2)$$

where φ_h is the amplitude of the initial state, and the summation is made over the entire reciprocal lattice. Individual terms of the sum are large only when the energy denominator is small. It is identically zero when both reciprocal lattice points H and H' lie on the sphere of reflection.

Three types of term can be seen to contribute to the intensity of the reflection h. The leading term for

$h-h'=0$ represents the amplitude of the diffracted wave when there are only two beams propagating in the crystal, and is proportional to V_h. A second distinct set of terms are those for which the energy denominator is identically zero, *i.e.* the strong simultaneous beams. The remaining contribution is from all the remaining reciprocal lattice points, *i.e.* the weak beams.

The elastic model then predicts that the variation of intensity of the specularly reflected beams as shown in the rotation diagram is a result of the exchange of current density among the various terms in the sum of equation (2). If one makes the approximation that the weak beam contribution is always small, then, since the contribution of the leading term is independent of the rotation, the first order effect is the exchange of current among the strong simultaneous reflections.*

As shown originally by Bethe (1928) the magnitude of V_h depends strongly on the magnitude of h: large V_h corresponds to small values of h. When V_h is small, or specifically zero, the summation over the strong simultaneous reflections can only make positive contributions to the intensity of the specularly reflected beam during the rotation. For the case where the magnitude of V_h is large, one can expect both positive and negative multiple diffraction peaks in the rotation diagram, as now the normal reflection V_h can contribute to the intensities of the weaker multiple reflections. Examination of the rotation diagram for 440, 550, 660, 770, 880, 990, show only positive contributions, while the 330 reflection shows mixed positive and negative contributions, indicating the relatively greater magnitude of V_{330}.†

* It must be borne in mind that above several hundred volts for most metals the elastic secondary current is of the order of 10% of the total secondary current and hence inelastic processes play a strong role in the diffraction process. We have measured the total secondary current as a function of voltage at constant angle during the intensity *versus* voltage curves, and at constant voltage during the intensity *versus* diffraction angle rocking curves. In both cases variations in the secondary current are observed, which in some instances can be correlated with variation in the elastic secondary current, indicating merely an exchange in elastic current between the forward and back scattering direction. On the other hand the rocking curves are accompanied by strong changes in the inelastic secondary current with angle, indicating strong changes in the inelastic processes accompanying the diffraction.

The total secondary current increases markedly for small values of the diffraction angle, presumably because the escape probability for low energy secondaries is large when they are produced near the surface as is the case for grazing incidence. Recent measurements of the variation of the total secondary current made during rocking curves for silver (Ducros & De Lafeuille, 1967) and made during both rotation diagrams and rocking curves for aluminum (DeBersuder, 1967) show very strong variations in the total inelastic secondary current as well. A detailed analysis of the total diffraction processes will be given in a forthcoming publication. Theoretical treatments of the inelastic process for high energy electron diffraction have been made by Yoshioka (1957) and Kanuma & Yoshika (1966).

† X-ray Renninger diagrams for these crystals show only positive multiple diffraction peaks for the 440 and higher reflections and mixed positive and negative peaks for the 330 and 220 reflections (Post, 1967).

Fractional order maxima

The foregoing discussion has served to demonstrate that the observed intensity maxima in the rocking curves are not integer order Bragg maxima, but are due to multiple diffraction, and hence exhibit first order dynamical effects. This argument can be extended to the other features of the rocking curves, especially the fractional order peaks which are generally observed. Fig. 8 shows the rotation diagram for the very weak half order reflection (6·5 6·5 0) shown in the [100] rocking curve of Fig. 2. For this geometry, $2\theta=90°$, and in the case of the rotation diagram the intensity of the fractional order peak appears only for the (110) orientation of the diffraction plane. In this case, the incident direction is [100]. The geometrical construction allows a determination of the multiple diffraction geometry, and only for the (110) orientation are several strong simultaneous reflections permitted, namely 224, 460 and 130.

The intensity of the reciprocal lattice rod (110) does not necessarily have a maximum at the fractional order position observed: the only requirement is that the intensity be non-zero at that point. The positions of the fractional orders in the rocking curve are only a function of the symmetry for multiple diffraction, which is dependent only on the orientation of the primary beam with respect to the reciprocal lattice, and is not connected with any property of the reciprocal lattice, except its symmetry. For different directions of incidence, other fractional orders appear whose intensities are related to the shape of the form factor, *i.e.* the appropriate values of $V_{h-h'}$. For the few directions of high symmetry studied, the fractional orders $1/(h^2+k^2+l^2)$ appear, when the incident beam is in the $[khl]$ direction. The cases for [100],[110],[111] are shown in Fig. 2, and up to $\frac{1}{8}$ orders have been observed.

The existence of such fractional orders has been pointed out by McRae (1966) for the case of normal incidence and for the general case by Boudreaux & Heine (1967).

At this point it is important to note that the gradual adsorption of the background gas ambient in the vacuum system completely eliminates the observed structure in the rotation diagrams, and the fractional order peaks in both the rocking curves and the intensity *versus* voltage plots. The extraordinary sensitivity of the multiple diffraction to the presence of adsorbed gas allows one to speculate as to the origin of the multiple diffraction structure.

One striking feature of the diffraction is that it contains intensities between the allowed Bragg positions, *i.e.* the half integer orders observed in the intensity *versus* voltage curves for the [110] direction. A mechanism for the extension of the reciprocal lattice is needed, but because of the large number of diffracting planes observed, a purely elastic mechanism based on the poor resolving power of the crystal is not possible (Boudreaux & Heine, 1967). We would like to propose

that this extension is quasielastic; *i.e.* it is due to phonon scattering, the energy loss being too small to detect.

Recent measurements (Stern & Baudoing, 1967) of the temperature dependence of the diffracted intensities show that the large amplitude of surface atomic vibrations is reduced* by the adsorption of many types of foreign atoms, and that this reduction is accompanied by the suppression of the fractional order diffraction maxima in the intensity *versus* voltage curves. Thus the presence of the multiple diffraction effects appears to be strongly tied to the vibrational spectrum of the surface atoms.

Detailed examination of the rotation diagrams shows no simple rule for determining the strength of a particular reflection $V_{h-h'}$. It is tempting to assume that because the surface of the crystal plays such an important role in the diffraction, surface reflections should be in some way exceptional. On this basis, one would expect the equatorial intersections of the sphere of reflection with the reciprocal lattice to exhibit special properties. Furthermore, if the reciprocal lattice is truly two-dimensional, and there is no intensity variation along the reciprocal lattice rods, only when such a rod enters or leaves the sphere of reflection should there be a change in the multiple diffraction condition. The importance of surface reflections (resonances) has been shown for alkali-halides (McRae & Caldwell, 1967), but the rotation diagrams described show no indication of these effects, although their existence at very low orders is not precluded. Furthermore, each intersection of the sphere of reflection with the expected position of a reciprocal lattice point is recorded in the rotation diagram indicating the presence of structure in the reciprocal lattice rods and the strong three-dimensional character of the diffraction.

* It is observed that the Debye–Waller factor is reduced, the angular spread of the diffraction feature is decreased and in addition the thermal diffuse features are suppressed.

Comparison with the two-beam model

This description of the effect of multiple diffraction is sufficiently complete to allow a comparison of the predictions of the model with those of the kinematical or two-beam description of the diffraction. The surprising result in the case where multiple diffraction predominates is the elimination of true Bragg peaks. In the two-beam model, the normal Bragg intensities are connected in a simple way with the diffraction properties of the lattice in a particular direction. For example, in the two-beam model the effective Debye temperature, as determined by the temperature dependence of the Bragg peak, is a measure of the amplitude of thermal vibration of a particular set of reflecting planes, while in the multiple diffraction case, it is a measure of the average vibrational amplitude in those directions given by a set of interactions for a given geometry. Its voltage dependence is therefore a measure of the way in which that average changes (Stern & Baudoing, 1967)*. The angular dependence of the Debye temperature now becomes a measurement of the way in which the multiple diffraction conditions change with incident angle rather than the way in which

* The Debye temperature measured for non-normal reflections appears to be anomalously large compared with the bulk value (Aldag & Stern, 1965; Stern & Baudoing, 1967). If multiple diffraction is dominant, then the normalization with respect to $\sin\theta/\lambda$ is incorrect because of the averaging over a range of angles, which leads to too large a value for θ_D.

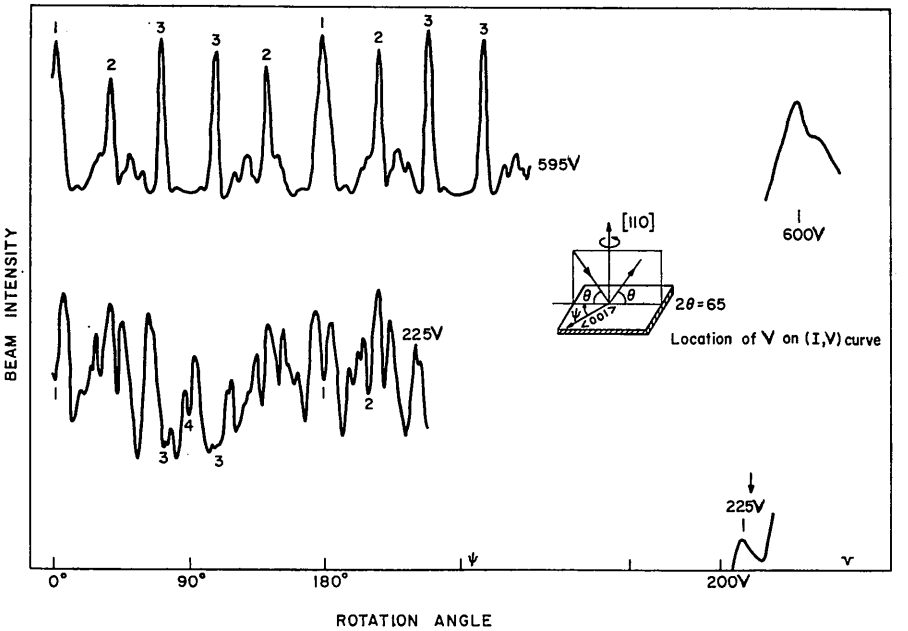

Fig. 6. Comparison of rotation diagrams for the 550 and the 330 reflections at $2\theta=65°$. The weak 550 reflection shows only positive multiple diffraction contributions, while the strong 330 reflection exhibits both negative and positive effects.

the vibrational amplitude changes with direction as interpreted by McRae (1965). The appearance of fractional orders in the rocking curve is not due to the shape of the reciprocal lattice determined by surface steps of defects,* but only to the multiple diffraction geometry. Since in the case of tungsten the relative contribution of the Bragg maxima for all but the lowest orders is nearly zero, all these interpretations must be considered in terms of the multiple diffraction case.

Inelastic anisotropy

The above discussion has been limited to the elastic part of the diffracted spectrum. The total secondary current contains strong variations in the distribution of electrons in both energy and momentum space. These variations have their origin in the dispersion relations for the various inelastic excitations possible in the crystal as the conservation laws place restrictions on the relationship between the change of energy and momentum for the electrons for a given excitation. Since a complete description of the scattering of electrons by a crystal must contain the details of the important interactions, it is of interest to look for anisotropy in inelastic excitations.

The apparently strong surface anisotropy of the phonon distribution in the (110) surface of tungsten (Aldag & Stern, 1965) evidently contributes second order dynamical effects to the overall anisotropy of the diffraction. In general, the experimental techniques used to measure the diffracted intensities allow sufficient energy resolution to permit the exclusion of electrons which have suffered inelastic scattering by all mechanisms, except phonon interactions which can only be eliminated by low temperature diffraction experiments.

It is possible to isolate certain regions of the inelastic spectrum which contribute significantly to the diffracted current. The energy loss characteristic of both the surface and bulk plasma excitations from the (110) tungsten surface have been observed (15 and 22 volts respectively) (Scheibner & Tharp, 1967). A difference between the rotation diagrams for elastic and inelastic electrons should indicate the anisotropy of those scattering mechanisms contained in the included energy range. Fig. 9 shows the elastic rotation diagram (lower curve) and the inelastic rotation diagram (upper curve) for a range of energies (about 50 volts) where the only scattering mechanisms expected to predominate are the plasma excitations.

In the purely elastic diffraction model, the rotation diagrams exhibit structure due to the exchange of intensity between the elastically diffracted beams. We have observed that the total secondary current also varies during the rotation, and that the inelastic diffracted current has a different angular dependence than the elastic current. A complete description of the diffraction must also consider the exchange of intensity be-

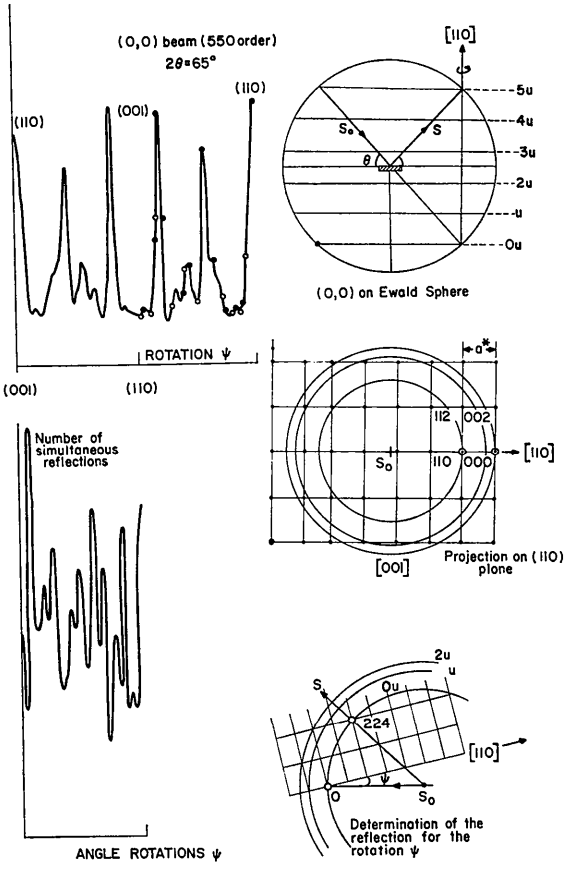

Fig. 7. Upper curve shows the rotation diagram from Fig. 3 with the appropriate geometry. The lower curve is proportional to the number of simultaneous reflections as a function of orientation. In the (110) orientation there are 20 simultaneous reflections. The construction geometry is indicated at the right.

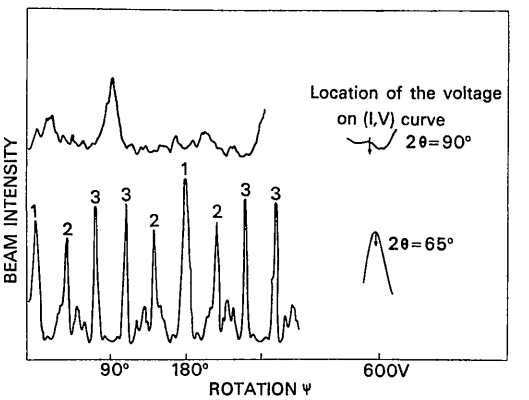

Fig. 8. Comparison of rotation diagram for integral and fractional order Bragg reflections. Lower curve: 550 reflection, $2\theta = 65°$, 595 eV; upper curve: 13/2, 13/2, 0 reflection, $2\theta = 90°$, 550 eV. The very weak half integer reflection has intensity only in the (110) orientation, which corresponds to a beam direction of [100].

* See, *e.g.* the papers on this subject in the Proceedings of the 1966 Durham Conference on the Structure of Surfaces, and The Proceedings of the 22nd MIT Physical Electronics Conference, 1967.

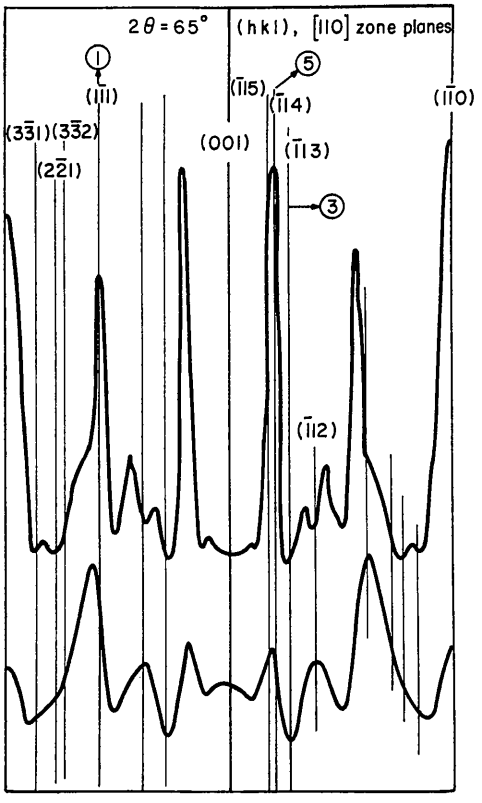

Fig. 9. Rotation diagram showing the difference between the intensity variation of the elastic beam excluding losses of more than three volts (lower curve) and the inelastic beam including losses of up to 60 volts. The rotation is from $\varphi=0$ to $\varphi=180°$, and the position of the low index planes of the [110] zone is indicated.

tween the elastic and inelastic spectrum, as well as the exchange between forward and backward elastic diffraction.

Conclusions

It has been shown that the intensities in low energy electron diffraction are due to the presence of strong dynamical interactions. In particular, the apparent Bragg maxima of both integral and non-integral order are completely anomalous on the basis of a two-beam kinematical model and have their origin in the symmetry conditions for multiple diffraction. As in X-ray and high energy electron diffraction, the dynamical theory is made possible by the knowledge of the details of the interaction of the several waves propagating in the crystal. In low energy electron diffraction this interaction is shown to be very important since there exist many simultaneous waves and the mutual interactions are strong. Because of the strength of the inelastic scattering mechanisms it is also necessary to consider the details of the latter, to explain the anisotropy of the diffraction completely. The danger of interpretation of diffraction effects on the basis of a two-beam kinematical model when strong dynamical effects are present is evident.

The authors wish to acknowledge helpful discussion with Prof. P. Ducros and K. Kambe.

References

ALDAG, J. P. & STERN, R. M. (1965). *Phys. Rev. Letters*, **14**, 857.
BETHE, H. A. (1928). *Ann. Phys.* **87**, 55.
BOUDREAUX, D. S. & HEINE, V. (1967). *Surf. Sci.* **8**, 426
BUNYAN, P. J. & SCHONFELDER, J. L. (1965). *Proc. Phys. Soc.* **85**, 455.
DARBYSHIRE, J. A. & COOPER, E. R. (1935). *Proc. Roy. Soc.* **A152**, 104.
DAVISSON, C. J. & GERMER, L. H. (1933). *Phys. Rev.* **33**, 760.
DEBERSUDER, L. (1967). Private communication.
DEICHSEL, H. & REICHERT, E. (1965). *Z. Physik*, **185**, 169.
DEICHSEL, H., REICHERT, E. & STEIDL, H. (1966). *Z. Physik*, **189**, 212.
DUCROS, P. & DE LAFEUILLE, D. (1967). Private communication.
EWALD, P. P. (1921). *Z. Kristallogr.* **56**, 129.
JAMES, R. W. (1962). *The Optical Principles of the Diffraction of X-Rays*. London: Bell.
KAMBE, K. (1967). *Z. Naturforsch.* **22a**, 422.
KANUMA, Y. & YOSHIKA, H. (1966). *J. Phys. Soc. Japan*, **21**, 1352.
KOSSEL, W. (1936). *Ann. Phys. Lpz.* **25**, 512.
LOTH, R. & ECKSTEIN, W. (1966). *Phys. Rev. Letters*, **20**, 390.
MCRAE, A. U. (1964). *Surf. Sci.* **2**, 522.
MCRAE, E. G. (1966). *J. Chem. Phys.* **45**, 3258.
MCRAE, E. G. & CALDWELL, C. W., JR. (1967). *Surf. Sci.* **7**, 41.
POST, B. (1967). Private communication.
RENNINGER, M. (1937). *Z. Physik*, **106**, 141.
SACCOCIO, E. J. & ZAJAC, A. (1966). *Phys. Rev.* **139**, A235.
SCHEIBNER, E. J. & THARP, L. N. (1967). Georgia Institute of Technology, Progress Report no. 6, Project B. 186. Proc. 1966 Durham Conf. on the Structure of Surfaces. Amsterdam: North-Holland Publishing Co.
STEIDL, H., DEICHSEL, H. & REICHERT, E. (1965). *Phys. Rev. Letters*, **17**, 31.
STERN, R. M. & BAUDOING. R. (1967). To be published.
TOURNAIRE, M. (1962). *J. Phys. Soc. Japan*, **17S-11**, 98.
YOSHIOKA, H. (1957). *J. Phys. Soc. Japan.* **12**, 618.
ZACHARIASEN, W. H. (1965). *Acta Cryst.* **18**, 765.
ZIMAN, J. M. (1960). *Electrons and Phonons*. Oxford: Clarendon Press.
ZIMAN, J. M. (1964). *Principles of the Theory of Solids*. Cambridge Univ. Press.